Inorg. Chem. **2005**, *44*, 4576–4585

Crystal Structure, Chemical Bonding, and Phase Relations of the Novel Compound $Co_4Al_{7+x}Si_{2-x}$ ($0.27 \leq x \leq 1.05$)

Klaus W. Richter,*,† Yurii Prots,‡ and Yuri Grin‡

Institut für anorganische Chemie, Universität Wien, Währingerstrasse 42, 1090 Wien, Austria, and Max-Planck-Institut für Chemische Physik fester Stoffe, Nöthnitzer Strasse 40, 01187 Dresden, Germany

Received November 22, 2004

The title compound was detected and characterized during a systematic study of the Al-rich part of the Co–Al–Si system. The crystal structure was established via single-crystal X-ray diffraction. It represents a new type of structure of intermetallic compounds (Pearson symbol *mC*26, space group *C*2/*m*). The homogeneity range of the phase $Co_4Al_{7+x}Si_{2-x}$ ($0.27(3) \leq x \leq 1.05(2)$) and equilibria with neighboring phases were studied by electron probe microanalysis (EPMA) and X-ray powder diffraction. The lattice parameters of the compound were found to vary between Al-poor and Al-rich composition (a = 11.949(1)–12.042(1) Å, b = 3.9986(4)–4.0186(4) Å, c = 7.6596(8)–7.6637(9) Å, and β = 106.581(7)–106.140(7)°). A partial disorder caused by the Al/Si substitution in one of the five main group element positions was found, and different ordering models yielding different Al/Si occupation motifs and different distributions of interatomic distances are discussed in detail. Chemical bonding analysis with the electron localization function (ELF) reveals a covalently bonded Al/Si network and rather ionic interactions between Co and the network.

Introduction

Ternary systems of iron group metals (M = Fe, Co, Ni) with aluminum and silicon are of great importance for many technical applications. A survey of current literature in the fields of materials science, metallurgy, and materials chemistry reveals a large number of research papers regarding stable and metastable phases in ternary Al−M−Si systems and their importance for the design and properties of advanced materials. Applied research activities in the systems mentioned include such different fields as high-temperature structural materials,[1] soft magnetic thin films and magnetic sheets,[2] constituent phases in commercial aluminum casting alloys[3] and hypereutectic Al−Si alloys,[4] thermoelectric power conversion,[5] and epitactic materials lattice matched to silicon.[6] Despite the broad interest in the applications for the systems, there is a significant lack of information on the structure, properties, and phase equilibria of the binary and ternary compounds in the respective systems. This is a result of several factors, including the complex character of phase equilibria, the occurrence of metastable phases, and insufficient basic research activities in the fields of phase characterization and phase diagram determination.

Al−M−Si compounds are also interesting from a very basic point of view because the careful investigation of the crystal structures in these compounds allows deeper insight into the chemical bonding in intermetallic compounds (the rationalization of which is, up to this point, far from complete) and into the mechanisms governing the formation of either ordered or partly disordered crystal structures. In fact, ternary compounds containing the combination of Al and Si are found to form extended solid−solution phases

* To whom correspondence should be addressed. Phone: +431 4277 52910. Fax: +431 4277 9529. E-mail: Klaus.Richter@univie.ac.at.
† Universität Wien.
‡ Max-Planck-Institut für Chemische Physik fester Stoffe.

(1) (a) Morris, D. G.; Nazmy, M.; Noseda, C. *Scr. Metall. Mater.* **1994**, *31*, 173. (b) Morris, D. G.; Gunther, S. *Acta Mater.* **1996**, *44*, 2847. (c) Golberg, D.; Demura, M.; Hirano, T. *Intermetallics* **1999**, *7*, 109. (d) Bosselet, F.; Viala, J. C.; Colin, C.; Mentzen, B. F.; Bouix, J. *Mater. Sci. Eng., A* **1993**, *167*, 147.
(2) Yoshida, S.; Sato, M.; Sugawara, E.; Shimada, Y. *J. Appl. Phys.* **1999**, *85*, 4636.
(3) (a) Mulazimoglu, M. H.; Zaluska, A.; Gruzleski, J. E.; Paray, F. *Metall. Mater. Trans. A* **1996**, *27*, 929. (b) Allen, C. M.; O'Reilly, K. A.; Cantor, B.; Evans, P. V. *Prog. Mater. Sci.* **1998**, *43*, 89. (c) Tanihata, H.; Sugawara, T.; Matsuda, K.; Ikeno, S. *J. Mater. Sci.* **1999**, *34*, 1205.
(4) (a) Kim, T. S.; Hong, S. J.; Kim, W. T.; Won, C. W.; Cho, S. S.; Chun, B. S. *Mater. Trans., JIM* **1998**, *39*, 1214. (b) Choi, Y. S.; Lee, J. S.; Kim, W. T.; Ra, H. Y. *J. Mater. Sci.* **1999**, *34*, 2163.
(5) (a) Ono, K.; Kado, M.; Suzuki, R. O. *Steel Res.* **1998**, *69*, 387. (b) Ohta, Y.; Miura, S.; Mishima, Y. *Intermetallics* **1999**, *7*, 1203.
(6) Richter, K. W.; Hiebl, K. *Appl. Phys. Lett.* **2003**, *83*, 497.

10.1021/ic0401243 CCC: $30.25
Published on Web 05/27/2005

Table 1. Structural Information on Ternary Phases in the Co−Al−Si System

phase	structure type	Pearson symbol, space group	lattice parameters (Å, deg)	unit cell volume (Å^3)	ref
α, $Co_3Al_{3-x}Si_{4+x}$	Ge_7Ir_3	*cI*40, $Im\bar{3}m$	$a = 8.075$	528.9	18
β, $Co_2Al_{1+x}Si_{2-x}$	Ni_2Al_3	*hP*5, $P\bar{3}m1$	$a = 3.867$ $c = 4.752$	61.54	18
γ, $Co_{19+x}Al_{43+y}Si_{12-y}$	own	*mC*296+, *C*2/*c*	$a = 20.040(3)$ $b = 19.170(3)$ $c = 12.826(1)$ $\beta = 123.591(8)$	4104.7(6)	19
δ, $Co_{32.5}Al_{40.5-43}Si_{22-24.5}$	own	*mC**	$a = 11.851(1)$ $b = 3.8838(4)$ $c = 7.4293(6)$ $\beta = 103.171(6)$	332.96(7)	19
ϵ, $Co_6Al_{11}Si_6$	own	*oC*184, *Cmc*2$_1$	$a = 8.0839(3)$ $b = 14.5445(6)$ $c = 21.354(1)$	2519.7(3)	19
χ, $Co_4Al_{7+x}Si_{2-x}$	own	*mC*26, *C*2/*m*	$a = 11.9935(8)$ $b = 4.0098(3)$ $c = 7.6590(8)$ $\beta = 106.357(6)$	353.4(1)	this work
ϕ, $Co_{10+x}Al_{25-x}Si_7$	own	*oP*168, *Pnma*,	$a = 13.846(2)$ $b = 23.050(2)$ $c = 7.336(1)$	2341.3(4)	19

on the basis of Al/Si substitution as well as ordered compounds with virtually no composition range. For example, the Al−Ni−Si system, recently studied in our group,[7] was found to contain a compound, $Ni_{16}Si_9Al$, with an ordered crystal structure (Pearson symbol *oC*104, space group *Cmcm*, new structure type) in the same composition area as several extended ternary solid−solution phases structurally unrelated to $Ni_{16}Si_9Al$. Careful investigation of this new structure type revealed that one particular position is occupied by aluminum together with silicon in a 1/1 ratio causing local symmetry breaking in the structure.[8]

The current paper is the first in a series of reports on the crystal structure and chemical bonding of newly characterized compounds in the Al-rich part of the Al−Co−Si system adjacent to the binary Al−Co system. In the Al-rich part of the Al−Co binary system, phase equilibria and crystal chemistry are quite complex. Six different phases have been found to exist in this region (≥70 at. % Al). These compounds are Co_2Al_9 (*mP*22, *P*2$_1$/c, Co_2Al_9 type)[9] and a bundle of three different phases around Co_4Al_{13} stoichiometry which are *o*-Co_4Al_{13} (*oP*102, *Pmn*2$_1$, *o*-Co_4Al_{13} type),[10] *m*-Co_4Al_{13} (*mC*102−7.2, *Cm*, *m*-Co_4Al_{13}),[11] and *h*-Co_4Al_{13} (also designated as Y-phase, *mC*34, *C*2/*m*, Os_4Al_{13} type).[12] The compound $CoAl_3$ (also designated as Z-phase or τ^2-Co_4Al_{13}) is reported to be decagonal quasicrystalline, and different approximate models have been given for this phase.[13] The hexagonal phase, Co_2Al_5 (*hP*28, *P*6$_3$/*mmc*, Co_2Al_5 type),[14] is the most Co-rich phase in the composition range under consideration. An important structural feature of these Al-rich compounds is the occurrence of condensed pentagonal prismatic channels, which are found in the Co_4Al_{13} phase bundle as well as in Co_2Al_5.[15] All of these structures can be considered to be closely related to the quasicrystals. The influence of the introduced silicon on this feature becomes of special basic interest.

Up to this point, only insufficient information about the structural chemistry of ternary Al−Co−Si compounds was available. A tentative ternary section of the system at 600 °C was given by German,[16] who reported the existence of 5 ternary phases. Two of them, α-$Co_3Al_{3-x}Si_{4+x}$ and *β*-$Co_2Al_{1+x}Si_{2-x}$, are structurally well described and exhibit considerable homogeneity ranges. The other three phases are designated as *γ*, *δ*, and *ϵ* and have not been structurally characterized up to this point. The compositions of these phases were reported to be $Co_{28}Al_{55}Si_{17}$ (*γ*), $Co_{33}Al_{44}Si_{23}$ (*δ*), and $Co_{30}Al_{42}Si_{28}$ (*ϵ*); they are all situated in the Al-rich corner of the phase diagram. The respective composition ranges were reported to be negligible.[16] However, in our own phase diagram investigation of the Al−Co−Si system, we found that phase equilibria in the Al-rich corner of the ternary system are even more complex and at least two additional compounds (*χ* and *ϕ*) could be identified in this composition area. Furthermore, the compositions of the structurally unidentified compounds, *γ*, *δ*, and *ϵ*, given by German et al.[16] deviate considerably from those found in our own study.[17] A compilation of the information about ternary phases in the Al−Co−Si system is given in Table 1. In this work, we report the crystal structure and phase relations of the novel ternary compound $Co_4Al_{7+x}Si_{2-x}$ ($0.27 \leq x \leq 1.05$) which is designated as the *χ* phase.

(7) (a) Richter, K. W.; Ipser, H. *Intermetallics* **2003**, *11*, 101. (b) Richter, K. W.; Chandrasekaran, K.; Ipser, H. *Intermetallics* **2004**, *12*, 545.
(8) Richter, K. W.; Prots, Yu.; Grin, Yu. *Z. Anorg. Allg. Chem.* **2004**, *630*, 417.
(9) (a) Douglas, A. M. B. *Acta Crystallogr.* **1950**, *3*, 19. (b) Boström, M.; Rosner, K.; Burkhardt, U.; Prots, Yu.; Grin, Yu. *Z. Anorg. Allg. Chem.* **2005**, *631*, 534.
(10) Grin, Yu.; Burkhardt, U.; Ellner, M.; Peters, K. *J. Alloys Compd.* **1994**, *206*, 243.
(11) (a) Hudd, R. C.; Taylor, W. H. *Acta Crystallogr.* **1962**, *15*, 441. (b) Burkhardt, U.; Ellner, M.; Grin, Yu. *Powder Diffr.* **1996**, *11*, 123.
(12) Gödecke, T.; Ellner, M. *Z. Metallkd.* **1996**, *87*, 854.
(13) (a) Li, X. Z.; Hiraga, K. *J. Alloys Compd.* **1998**, *269*, L13. (b) Ma, X. L.; Kuo, K. H. *Metall. Mater. Trans. A* **1992**, *23*, 1121.
(14) (a) Newkirk, J. B.; Black, P. J.; Damjanovich, A. *Acta Crystallogr.* **1961**, *14*, 532. (b) Burkhardt, U.; Ellner, M.; Grin, Yu.; Baumgartner, B. *Powder Diffr.* **1998**, *13*, 159.
(15) Grin, Yu.; Burkhardt, U.; Ellner, M.; Peters, K. *Z. Kristallogr.* **1994**, *209*, 479.
(16) German, N. V. *Vestn. L'vov. Univ. Chim.* **1981**, *23*, 61.
(17) Richter, K. W.; Tordesillas Gutiérrez, D. *Intermetallics* **2005**, *13*, 848.

Experimental Section

The title compound was observed in a series of samples at 28, 30, 32, and 34 at. % Co with Si contents varying between 4 and 20 at. %. Samples were prepared from cobalt pieces (purity grade 99.9+%, Alfa), aluminum (99.999%, Alfa), and silicon rod (99.9999%, Dow Corning). Calculated amounts of the elements were weighed with an accuracy of 0.05 mg and arc melted on a water-cooled copper plate under an argon atmosphere. Zirconium was used as a getter material. The reguli, with a total mass about 1000 mg, were remelted one or two times for homogenization and then reweighed to check for possible mass losses, which were found to be negligible (less than 1 mg). The reguli were subsequently placed in alumina crucibles which were sealed into evacuated quartz glass ampules. The ampules were heated to 1050 °C within a day and then cooled slowly (5 K h^{-1}) to 800 °C in order to promote crystal growth from the melt. The homogenization annealing was performed at 800 °C for 4 weeks. After the samples were quenched in cold water, they were divided into several pieces and investigated by X-ray powder diffraction (XRD), electron microprobe analysis (EPMA), and metallographical analysis. No reaction of the samples with the alumina could be detected.

Initial sample characterization was performed by X-ray powder diffraction using a Guinier camera (Huber G670) equipped with an image plate detection system and employing Co Kα_1 radiation (λ = 1.78896 Å). Lanthanum hexaboride, LaB_6 (a = 4.15692(1) Å), was used as an internal standard for lattice parameter determination.

Polished pieces of the annealed samples were investigated by optical microscopy using a Zeiss Axiotech 100 microscope equipped for operation with polarized light. Selected samples were then analyzed by EPMA to determine reliable compositions of the title compound and the various phases found in equilibrium with it. The EPMA measurements were carried out on a Cameca SX 100 electron probe analyzer using wavelength dispersive spectroscopy (WDXS) for quantitative analysis and employing elemental aluminum, silicon, and cobalt as standard materials. The measurements were carried out at 15 kV with a beam current of 20 mA. A conventional ZAF matrix correction was used to calculate the final composition.

The crystal structure investigation was carried out on two single-crystal specimens mechanically extracted from the annealed samples with different nominal compositions ($Co_{28}Al_{64}Si_8$ and $Co_{30}Al_{54}Si_{16}$), both situated slightly outside the exact homogeneity range of the χ phase and thus containing small amounts of neighboring compounds. As both refinements revealed very similar results only one of the data sets ($Co_{28}Al_{64}Si_8$) is used for the discussion of the structure. The intensity data were collected on a Rigaku AFC7 diffractometer system equipped with a Mercury CCD detector. In each case, two measurements with long and short exposure times were performed to obtain accurate intensities for the strong and weak reflections. Both data sets were scaled and combined using the XPREP program.[20] All crystallographic calculations were performed with the WinCSD program package.[21] Relevant data concerning data collection and crystal structure refinement are summarized in Table 2.

Table 2. Crystallographic Information, Data Collection, and Handling for $Co_4Al_{7+x}Si_{2-x}$ (x = 0.75)

formula	$Co_4Al_{7.75}Si_{1.25}$
crystal size (mm^3)	0.065 × 0.100 × 0.120
diffractometer	Rigaku AFC7
detector	Mercury CCD
radiation, λ (Å)	Mo Kα, 0.71070
scans, step	φ/ω, 0.6°
number of images	500
2θ range up to	67.67°
space group, Pearson symbol	$C2/m$ (no. 12), $mC26$
unit cell parameters[a]	
a (Å)	11.9935(8)
b (Å)	4.0098(3)
c (Å)	7.6590(8)
β (deg)	106.357(6)
V ($Å^3$)	353.4(1)
formula units/cell, Z	2
ranges for h, k, l	$-18 \le h \le 18$
	$-4 \le k \le 6$
	$-11 \le l \le 10$
$N(hkl)$ measured/unique	2312/683
R(int)	0.030
$N(hkl)$ observed ($F(hkl) > 4\sigma(F)$)	666
refined parameters	44
$R(F)$[b]	0.030
extinction parameter	0.0132(7)
max. residual density peak ($e/Å^3$)	+1.45

[a] Lattice parameters calculated from Guinier powder data using LaB_6 (a = 4.15692 Å) as the standard. [b] $R(F) = \sum(|F_o| - |F_c|)/\sum|F_o|$.

Quantum Chemical Calculations

The TB-LMTO-ASA program package[22] with Barth and Hedin's[23] exchange correlation potential (LDA) was used for the quantum chemical calculations. The calculation was performed for the ordered model $Co_4Al_7Si_2$ with full silicon occupancy for the Si/Al site and Al4 in the 2d site. The radial scalar-relativistic Dirac equation was solved to get the partial waves. Although the calculation within the atomic sphere approximation (ASA) includes corrections for the neglect of the interstitial regions and partial waves of higher order,[24] an addition of empty spheres in the case of $Co_4Al_7Si_2$ was not necessary. The following radii of atomic spheres were applied for calculations: r(Co1) = 1.371 Å, r(Co2) = 1.420 Å, r(Si) = 1.419 Å, r(Al1) = 1.568 Å, r(Al2) = 1.540 Å, r(Al3) = 1.561 Å, and r(Al4) = 1.439 Å. A basis set containing Al(3s,3p), Co(4s,4p,3d), and Si(3s,3p) orbitals was employed for the self-consistent calculations with the Al(3d) and Si(3d) functions being downfolded.

The electron localization function (ELF, η) was evaluated according to Savin et al.[25] with an ELF module already implemented within the TB-LMTO-ASA program package. The topology of ELF was analyzed with the program Basin[26] to gain a deeper insight into the chemical bonding. The electron density was integrated in basins which are bounded by zero-flux surfaces in the ELF gradient field. This method is analogous to the procedure proposed by Bader for the electron density.[27] The resulting electron counts for each basin reveal basic information for the description of the bonding situation.

(18) Schmid-Fetzer, R. In *Ternary Alloys*; Petzow, G., Effenberg, G., Eds.; VCH: Weinheim, Germany, 1991; p 254.
(19) Richter, K. W.; Prots, Yu.; Grin, Yu. Publication in preparation.
(20) Sheldrick, G. *XPREP—Data Preparation and Reciprocal Space Exploration*, version 5.1; Bruker AXS: Madison, WI, 1997.
(21) Akselrud, L. G.; Zavalij, P. Y.; Grin, Yu. N.; Pecharsky, V. K.; Baumgartner, B.; Wölfel, E. *Mater. Sci. Forum* **1993**, *133—136*, 335.
(22) Jepsen, O.; Burkhardt, A.; Andersen, O. K. *TB-LMTO-ASA*, version 4.7; Max-Planck-Institut für Festkörperforschung: Stuttgart, Germany, 1999.
(23) Barth, U.; Hedin, L. *J. Phys. C* **1972**, *5*, 1629.
(24) Andersen, O. K. *Phys. Rev. B* **1975**, *12*, 3060.
(25) Savin, A.; Flad, H. J.; Flad, J.; Preuss, H.; von Schnering, H. G. *Angew. Chem.* **1992**, *104*, 185; *Angew. Chem., Int. Ed. Engl.* **1992**, *31*, 185.
(26) Kohout, M. *Basin*, version 2.3; Max-Planck-Institut für Chemische Physik fester Stoffe: Dresden, Germany, 2001.
(27) Bader, R. F. W. *Atoms in Molecules: A Quantum Theory*; Oxford University Press: Oxford, U.K., 1999.

Table 3. Composition of the $Co_4Al_{7+x}Si_{2-x}$ Phase in Various Phase Fields

nominal sample composition	phase field	composition of the $Co_4Al_{7+x}Si_{2-x}$ phase
$Co_{28}Al_{64}Si_8$	$\chi + \gamma + (CoAl_3)$	$Co_{30.8(2)}Al_{59.6(2)}Si_{9.6(2)}$
$Co_{30}Al_{58}Si_{12}$	$\chi + \gamma$	$Co_{30.5(1)}Al_{58.2(1)}Si_{11.3(1)}$
$Co_{30}Al_{54}Si_{16}$	$\chi + \gamma + \delta$	$Co_{30.4(1)}Al_{56.3(2)}Si_{13.3(2)}$
$Co_{34}Al_{58}Si_8$	$\chi + (CoAl)$	$Co_{30.9(1)}Al_{61.8(1)}Si_{7.3(1)}$
$Co_{34}Al_{54}Si_{12}$	$\chi + (CoAl)$	$Co_{30.7(1)}Al_{58.6(1)}Si_{10.7(1)}$
$Co_{34}Al_{50}Si_{16}$	$\chi + \beta$	$Co_{30.7(1)}Al_{56.6(1)}Si_{12.7(1)}$
$Co_{34}Al_{46}Si_{20}$	$\chi + \beta + \delta$	$Co_{30.7(2)}Al_{56.2(2)}Si_{13.1(2)}$

Results and Discussion

After the initial observation of the previously unknown powder pattern of the χ phase in a sample with the nominal composition $Co_{28}Al_{64}Si_8$, a systematic scan of the corresponding composition area was performed to determine the phase equilibria and homogeneity range of the χ phase. Phase relations of the χ phase were determined by a combination of powder XRD and EMPA analysis. The respective experimental composition data from EPMA are given in Table 3 together with the nominal sample composition and the phases present in equilibrium with the χ phase. The compositions are normalized to 100 at. %. The amount of Co in the χ phase is almost constant in the different two- and three-phase regions (30.7 at. % in average) and corresponds very well with the cobalt content of 30.8 at. % calculated from the formula $Co_4Al_{7+x}Si_{2-x}$, which was the result of the crystal structure investigation (see below). In contrast to the constant Co content observed in the χ phase, a considerable homogeneity range was found from the Al/Si ratio. The respective limiting compositions determined by EPMA are in the range of 7.3(1)−13.3(2) at. % Si (Table 3) corresponding to the homogeneity range of $0.27(3) \leq x \leq 1.05(2)$.

X-ray powder diffraction was used to investigate the variation of the lattice parameters with the composition (Si/Al ratio) on selected samples with phase compositions characterized by EPMA. The variation of the *a* and *b* parameters is considerable, whereas the *c* parameter does not show any significant change with the composition (Figure 1). The trend of the volume change is consistent with the radii of Al and Si (atomic radii $r(Al) = 1.43$ Å, $r(Si) = 1.17$ Å; covalent radii $r(Al) = 1.25$ Å, $r(Si) = 1.17$ Å),[28] and the almost linear variation of the volume with the composition suggests a simple Al/Si substitution mechanism for homogeneity range formation.

The crystal structure of $Co_4Al_{7+x}Si_{2-x}$ was determined on a single crystal selected from the sample with nominal composition $Co_{28}Al_{64}Si_8$ containing the χ phase with measured composition $Co_{30.8(2)}Al_{59.6(2)}Si_{9.6(2)}$ ($Co_4Al_{6.75}Si_{1.25}$) together with small amounts of the γ and $CoAl_3$ phases (Table 3). The analysis of the single-crystal diffraction data clearly indicated Laue class 2/*m* and a *C*-centered Bravais lattice. From the three possible space groups, *C*2, *Cm*, and *C*2/*m*, the centrosymmetric one was found to be correct during the structure determination and refinement. The initial model was established with direct methods (all of the Co and part of the Al positions), and the remaining atomic sites were identified from the difference Fourier map. Originally, seven crystallographically independent sites could be identified: two Co and five main group element positions, which were preliminarily refined as occupied with aluminum. All atomic sites are situated within the mirror planes at $y = 0$ and $y = 1/2$. Subsequently all atomic positions were refined with anisotropic displacement parameters. At this stage, it was observed that Al4, which was originally refined at the 2d position (1/2, 0, 1/2; site symmetry 2/*m*), showed unreasonable anisotropic behavior ($B_{11}/B_{22}/B_{33} \approx 5/1/3$, Figure 2). From the difference Fourier map (Figure 3, bottom), a split model with a half-occupied 4i position (site symmetry *m*) was developed for Al4. Refinement with a fixed isotropic displacement parameter for this position yielded reasonable displacement parameters in the subsequent anisotropic

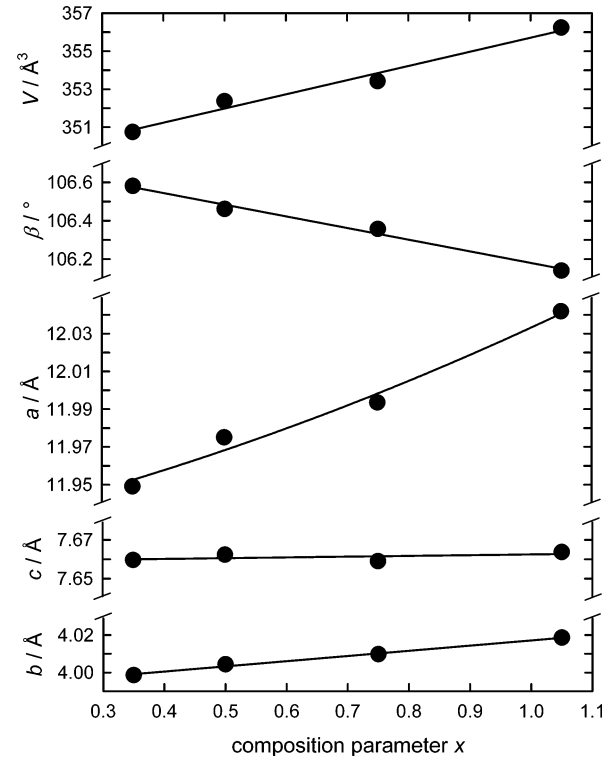

Figure 1. Variation of the lattice parameters and the unit cell volume of $Co_4Al_{7+x}Si_{2-x}$ with the composition obtained from different two- and three-phase samples. The composition parameter, *x*, was determined by EPMA measurements.

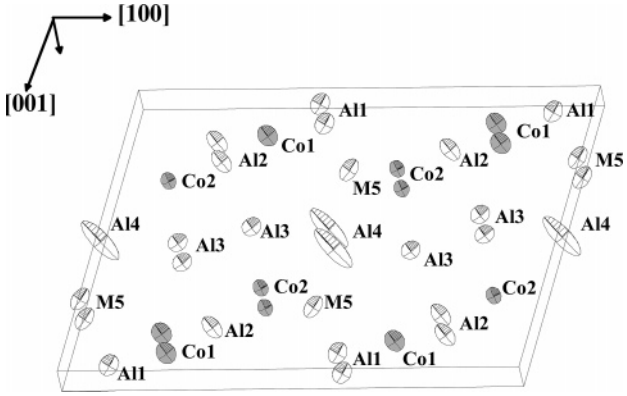

Figure 2. Displacement ellipsoids at the 97% probability level of atoms in the structural model of $Co_4Al_{7+x}Si_{2-x}$ without positional splitting.

(28) Emsley, J. *The Elements*; Walter de Gruyter: Hawthorne, NY, 1994.

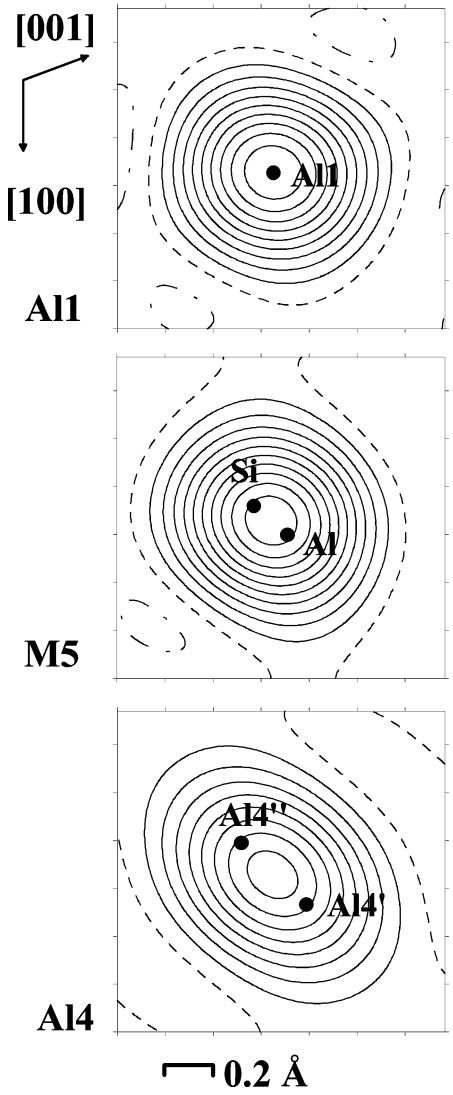

Figure 3. Difference electron density map in the vicinity of positions Al1 (not split), Al4, and M5. The black dots indicate the refined atomic positions.

refinement. The splitting observed in Al4 is closely related to the special coordination environment of this position. Al4 is surrounded by eight Al/Si atoms forming a distorted rectangular prism with two faces capped by Co2 atoms. The distance to the two Co2 neighbors is very short (2×2.358 Å). In contrast, in the direction of the anisotropic distortion (i.e., the direction of the observed splitting) the distance to the next neighbor (Al2) is very large (3.70 Å) and thus does not restrict the shift out of the special 2d position (Figure 4). The shift slightly reduces the tight distance to Co2 and splits the distances to the Al/Si atoms into two sets.

In the next step, splitting was also considered for the M5 position which was found to be the most likely for Al/Si substitution (Figure 3, middle). The observed homogeneity range of $Co_4Al_{7+x}Si_{2-x}$ ($0.27 \leq x \leq 1.05$) clearly indicates Al/Si substitution. As the scattering factors of Al and Si are rather similar and thus an unambiguous identification of Al or Si by refinement is difficult, our occupation model is primarily based on the analysis of the interatomic distances. Given the considerable size difference between Al and Si, it is safe to assume that Si will preferably enter the site with

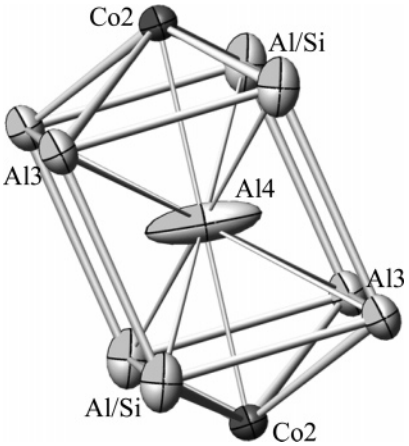

Figure 4. Environment of the Al4 position with bonds up to 3.1 Å shown.

the shortest distances to the neighboring atoms. This position exhibits three very close contacts to Co atoms and a number of close aluminum positions. The refinement allowing mixed Al/Si occupation in the M5 position and splitting gave reasonable distances for Al and Si, and the free refinement of the occupation numbers yielded a convincing result for the overall composition. For comparison, the difference electron density deformation around the Al1 position (not split) with the two split positions is shown in Figure 3. Final atomic coordinates and displacement parameters are given in Table 4. For the interatomic distance calculations, lattice parameters obtained from the least-squares refinement of 32 reflections extracted from the X-ray powder pattern of the bulk sample $Co_{28}Al_{64}Si_8$ were used. Selected interatomic distances are presented in Table 5. The refined composition $Co_4Al_{7.8(2)}Si_{1.3(2)}$ is in perfect agreement with the corresponding value of $Co_4Al_{7.75(2)}Si_{1.25(2)}$ determined by EPMA.

Both split positions (Al4 and M5) reflect the partial disorder in the vicinity of the 2d site in the crystal structure of $Co_4Al_{7+x}Si_{2-x}$. Locally, this disorder can be described with ordered models with different occupations of the Al4′/Al4″ and M5 (Al/Si) positions. Figure 5 shows that these models also differ in the number of short interatomic distances between crucial positions (for definition of the short distances see below). If the Si and Al4′ positions are occupied, the Si atoms have seven nearest neighbors (Figure 5a), and in case of Al and Al4″ occupation, the Al atoms have eight nearest ligands (Figure 5b). In the two other cases (Figure 5c, d), the silicon atoms have six or eight nearest neighbors, and the aluminum atoms have eight or nine closest ligands. In all of these models, the total coordination number of the Al/Si position is in fact ten, if the longer interatomic distances are also considered (Figure 5, right side, and Table 5), and the central atoms (Al or Si) always have three Co neighbors.

The structure type of $Co_4Al_{7+x}Si_{2-x}$ is unique and surprisingly does not show an obvious close relationship to any of the neighboring binary Co−Al phases or to the structurally characterized Al-rich phases in the Al−Fe−Si system like $Fe_5Al_{12}Si_3$ (*hP*26, $P6_3/mmc$, Mn_3Al_{10} type).[29] A common structural feature of the adjacent binary phase Co_2Al_5 and

(29) Zarechnyuk, O. S.; German, N. V.; Yanson, T. I.; Rykhal, R. M.; Murav'eva, A. A. *Fazovye Ravnovesiya Met. Splavakh* **1981**, 69.

Table 4. Atomic Coordinates and Displacement Parameters (in 10^4 Å^2) for $Co_4Al_{7+x}Si_{2-x}$ ($x = 0.75$)

atom	site	x	y	z	U_{11}	U_{22}	U_{33}	U_{13}	U_{iso}[a]
Co1	4i	0.79744(5)	0	0.13160(9)	81(3)	68(3)	78(3)	31(2)	74(2)
Co2	4i	0.61080(5)	0	0.28984(8)	47(3)	68(3)	48(3)	18(2)	54(2)
Al1	4i	0.4027(1)	0	0.0552(2)	58(6)	58(6)	76(6)	4(5)	67(4)
Al2	4i	0.2026(1)	0	0.1869(2)	92(6)	36(5)	94(6)	55(5)	68(4)
Al3	4i	0.8197(1)	0	0.4554(2)	65(6)	105(6)	54(5)	3(5)	78(4)
Al4[b]	4i	0.5139(2)	0	0.5183(5)	77(15)	78(9)	65(13)	30(13)	71(8)
Si[b]	4i	0.9941(4)	0	0.266(2)					63(5)[c]
Al[b]	4i	0.9981(10)	0	0.247(3)					60(9)[c]

[a] $U_{12} = U_{23} = 0$. [b] Occupancies: Al4, 0.50 (fixed); Si, 0.66(11); Al, 0.38(11). [c] The split (M5) positions Al/Si were refined with isotropic displacement parameters.

Table 5. Selected Interatomic Distances for $Co_4Al_{7+x}Si_{2-x}$ ($x = 0.75$)

atoms		distance	atoms		distance
Co1	−Si[a]	2.293(8)	Al3	−Co1	2.418(2)
	−Al[a]	2.32(2)		−Co2	2.469(2)
	−2Al2	2.4011(9)		−Si[a]	2.617(10)
	−Al3	2.418(2)		−Al[a]	2.68(2)
	−Al1	2.423(2)		−2Co2	2.758(1)
	−Al2	2.440(2)		−Al4[a]	2.796(2)
	−2Al1	2.524(1)			3.007(3)
	−Co2	2.8298(9)		−Al3	2.816(2)
	−Co1	2.8435(6)		−Al2	2.827(2)
Co2	−Al4[a]	2.358(3)		−Si[a]	2.860(8)
		2.373(3)		−Al[a]	3.01(2)
	−2Al[a]	2.388(8)		−2Al2	2.931(2)
	−2Si[a]	2.422(4)	Al4[a]	−Co2	2.358(3)
	−Al3	2.469(2)		−Co2	2.373(3)
	−Al2	2.518(1)		−2Si[a]	2.615(8)
	−Al2	2.518(1)		−2Al[a]	2.72(2)
	−Al1	2.602(2)		−2Si[a]	2.747(8)
	−Al1	2.633(2)		−2Al[a]	2.85(2)
	−2Al3	2.758(1)		−2Al3	2.796(2)
	−Co1	2.8298(9)		−2Al3	3.007(3)
Al1	−Co1	2.423(2)	Al[a]	−Co1	2.32(2)
	−2Co1	2.524(1)		−Co2	2.388(8)
	−2Al[a]	2.558(15)		−Co2	2.388(8)
	−2Si[a]	2.615(7)		−2Al1	2.558(15)
	−Co2	2.602(2)		−Al2	2.620(14)
	−Co2	2.633(2)		−Al3	2.68(2)
	−Al1	2.698(2)		−2Al4[a]	2.72(2)
	−Al2	2.781(1)			2.85(2)
	−Al2	2.853(2)		−Al3	3.01(2)
Al2	−2Co1	2.4011(9)	Si[a]	−Co1	2.293(8)
	−Co1	2.440(2)		−Co2	2.422(4)
	−2Co2	2.518(1)		−Co2	2.422(4)
	−Al[a]	2.620(14)		−2Al1	2.615(7)
	−Si[a]	2.734(7)		−2Al4[a]	2.615(8)
	−2Al1	2.781(1)			2.747(8)
	−Al3	2.827(2)		−Al3	2.617(10)
	−Al1	2.853(2)		−Al2	2.734(7)
	−2Al3	2.931(2)		−Al3	2.860(8)

[a] Split positions.

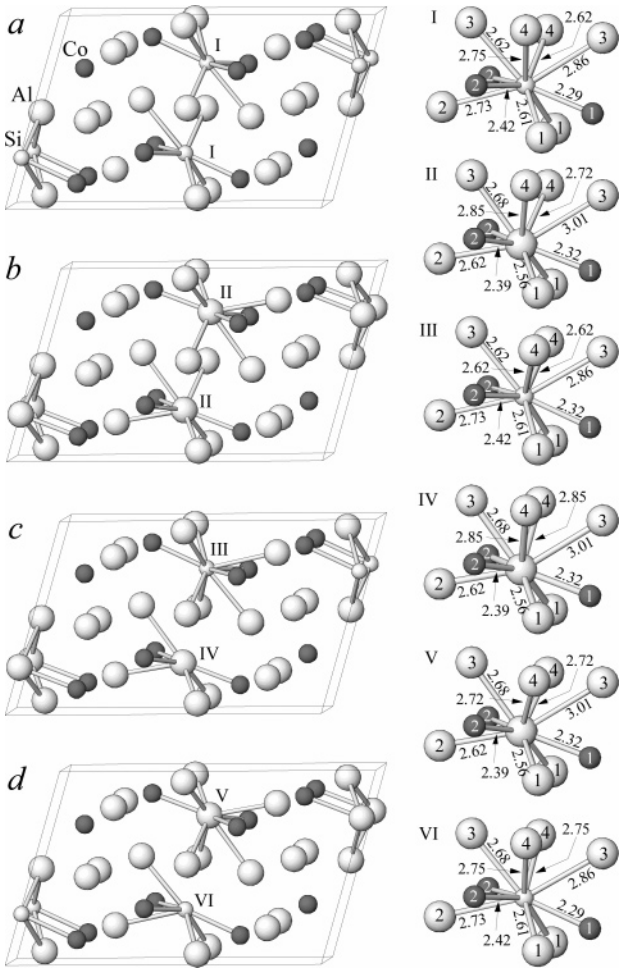

Figure 5. Different ordering models for the region around positions Al4 and M5 (a−d). Short interatomic distances around the Al/Si positions are shown ($d_{Al-Al} \leq 2.80$ Å; d_{Co-Al}, d_{Co-Si}, $d_{Si-Al} \leq 2.65$ Å). Coordination polyhedra of the M5 (Al or Si) position (I−VI) with interatomic distances to ligand atoms (in Å). The numbers inside the circles represent the atom designations as found in Table 4.

the phase bundle around Co_4Al_{13} is the occurrence of condensed pentagonal prismatic channels which are centered by Co and Al atoms and show different arrangements (pair connected or condensed to slabs) within the respective unit cells.[11] This structural relation has been discussed on a much broader basis, including a number of transition-metal aluminides and gallides, such as V_2Ga_5, Fe_2Al_5, V_7Al_{45}, V_4Al_{23}, and VAl_{10}, which all show one-dimensional infinite pentagonal channels.[15] The structure of the quasicrystalline decagonal $CoAl_3$ is also based on the typical local environment of the cobalt atoms with pentagonal or pseudopentagonal symmetry.[13] This kind of atomic arrangement is missing in the crystal structure of $Co_4Al_{7+x}Si_{2-x}$ which, de facto, does not show icosahedral or pentagonal prismatic coordination for any of the Co or Al (Si) sites (Figure 6).

The coordination polyhedra observed in $Co_4Al_{7+x}Si_{2-x}$ are best understood by the stacking of flat layers in $y = 0$ and $y = 1/2$ as shown in Figure 7. As all of the atomic positions of the $Co_4Al_{7+x}Si_{2-x}$ structure are situated in the special 4i position of the space group $C2/m$ (site symmetry m), the layers in $y = 0$ and $y = 1/2$ show the identical atomic arrangement shifted by $a/2$ because of the the C-entering of the lattice. Therefore, all of the coordination polyhedra may be visualized as trigonal or distorted rectangular prisms with

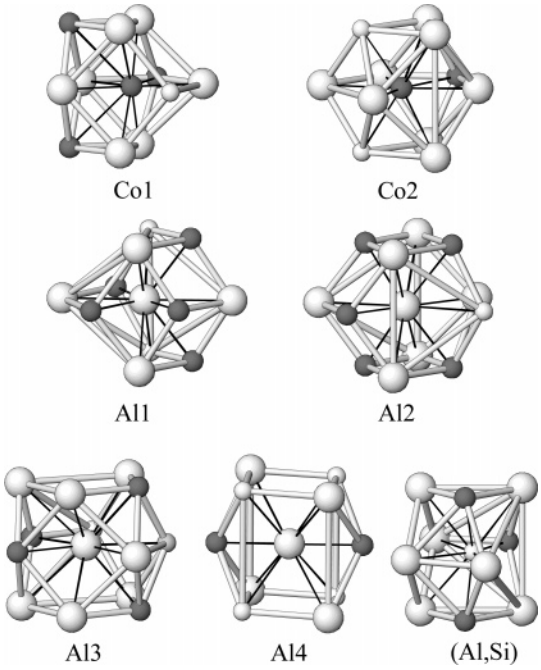

Figure 6. Coordination polyhedra of the atomic positions in the crystal structure of $Co_4Al_{7+x}Si_{2-x}$.

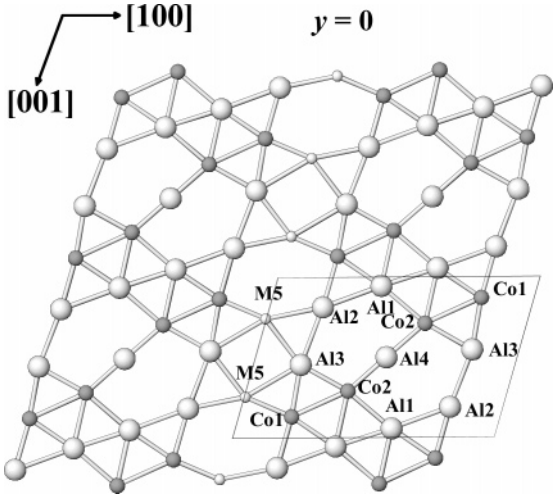

Figure 7. Arrangement of atoms within the flat layers at $y = 0$ in the crystal structure of $Co_4Al_{7+x}Si_{2-x}$. The layers in $y = 1/2$ show the identical atomic arrangement shifted by $a/2$ because of the C-entering of the lattice.

2, 4, or 5 additional vertexes in front of the side faces of the prisms, yielding coordination numbers between 10 and 13 (Figure 6). The coordination of the cobalt atoms is the only significant connection between the title compound and the adjacent binary compounds; the trigonal prisms with 5 additional vertexes can also be found in *o*-Co_4Al_{13} and Fe_4Al_{13}.[10,15] This similarity can be seen in Figure 8 (left down) which shows some of the typical coordination polyhedra of transition metal atoms in Al-rich binary compounds.

Thus, the common structural motif in the crystal structures of the chemically related compounds $Co_4Al_{7+x}Si_{2-x}$, *o*-Co_4Al_{13}, and Fe_4Al_{13} is not the pentagonal atomic arrangement but a "cluster" formed from the two trigonal prisms around cobalt (transition metal) and a distorted rectangular prism around the aluminum (Figure 9). In $Co_4Al_{7+x}Si_{2-x}$, they

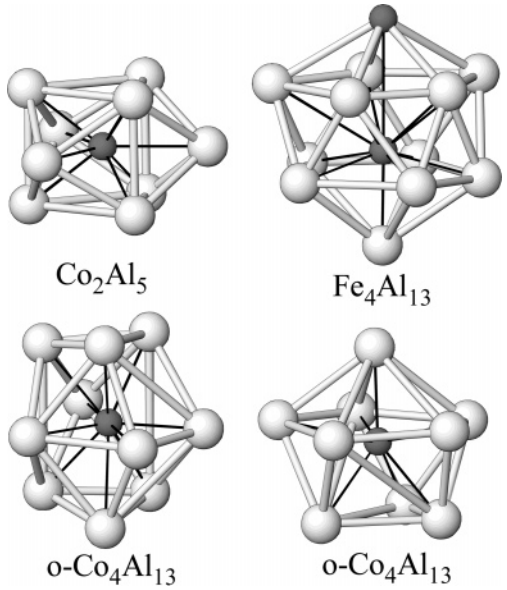

Figure 8. Coordination of selected transition metal positions in Co_2Al_5, Fe_4Al_{13}, and *o*-Co_4Al_{13} showing the typical coordination environments of the transition metals in Al-rich binary compounds.

show up as isolated, not connected to each other. In both binary compounds, they are partially condensed via the vertexes of the trigonal prisms. The remaining part of the crystal structures of *o*-Co_4Al_{13} and Fe_4Al_{13} is formed by the atomic arrangements with local pseudopentagonal symmetry mentioned above. In the crystal structure of $Co_4Al_{7+x}Si_{2-x}$, the remaining part does not show this feature. The introduction of larger cations, such as rare earth or alkaline earth metals, in addition to the transition metals leads to the further condensation of such clusters and to the formation of infinite bands in ternary compounds with the crystal structures of the $CeFe_2Al_8$[30] and $LaCoAl_4$[31] types. Here, the remaining part of the structure may be best visualized by an infinite pentagonal prismatic channel of Al atoms centered by the rare earth element (Ce, La) and, in the case of $CeFe_2Al_8$, by Al (Figure 9). Thus, the implementation of a relatively small amount of silicon seems to suppress the formation of the atomic arrangements with pseudopentagonal symmetry in the crystal structures of ternary compounds in comparison with that of the binary aluminides of cobalt and iron.

Common clusters can be also visualized by comparing the crystal structure of $Co_4Al_{7+x}Si_{2-x}$ with that of another chemically related compound, Os_4Al_{13}, which is also the structure type of *h*-Co_4Al_{13}.[32] As shown in Figure 10, these clusters are also formed by polyhedrons around cobalt (or osmium) atoms. Two polyhedrons of the Co2 share the Al1−Al1 edge, forming an empty distorted cube in between. In the crystal structure of $Co_4Al_{7+x}Si_{2-x}$, these clusters are isolated and stacked along the [100] axis. The remaining space is filled by polyhedrons of Co2 and Al4 (Figure 10, top). The crystal structure of Os_4Al_{13} can be described as

(30) Yarmolyuk, Ya. P.; Rykhal, R. M.; Zarechnyuk, O. S. *Second All-union Conference on Crystal Chemistry of Intermetallic Compounds*; Lvov, Ukraine, 1974; p 39.
(31) Rykhal, R. M.; Zarechnyuk, O. S.; Yarmolyuk, Ya. P. *Dop. Nats. Akad. Nauk Ukr. A* **1977**, *39*, 265.
(32) Edshammer, L. E. *Acta Chem. Scand.* **1964**, *18*, 2294.

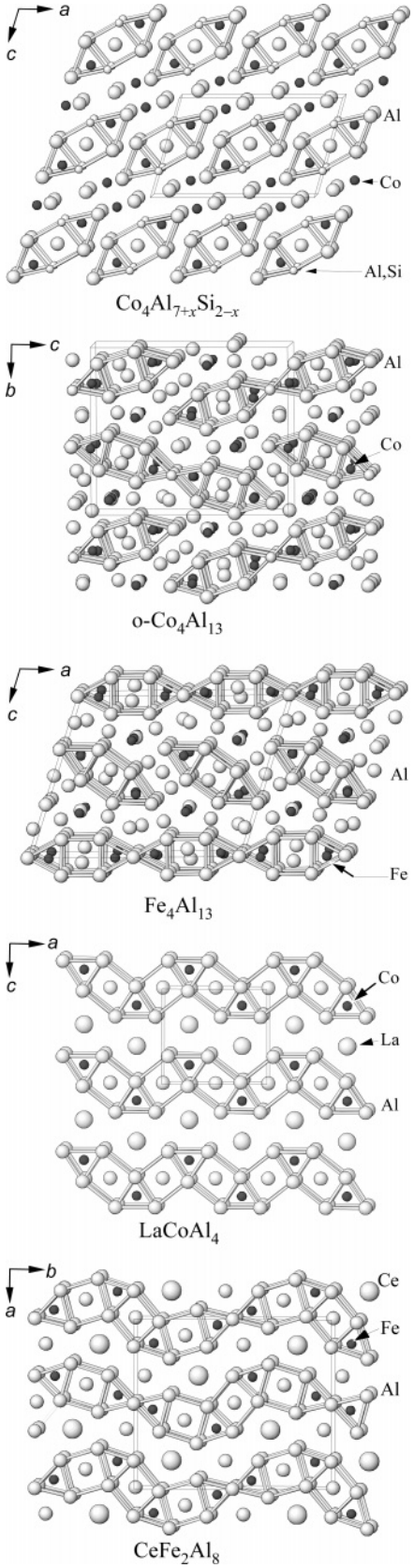

Figure 9. Arrangement of the common atomic clusters containing trigonal prisms centered by Co(Fe) and distorted rectangular prisms centered by Al in the crystal structures of $Co_4Al_{7+x}Si_{2-x}$, *o*-Co_4Al_{13}, Fe_4Al_{13}, $LaCoAl_4$, and $CeFe_2Al_8$.

having the whole space filled by the clusters described above. They are condensed to chains along the [001] axis sharing

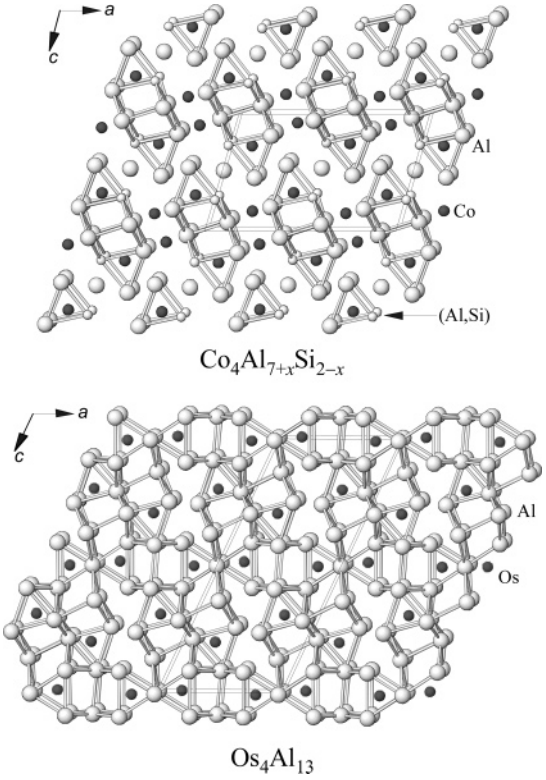

Figure 10. Arrangement of the common atomic clusters in the crystal structures of $Co_4Al_{7+x}Si_{2-x}$ (top) and Os_4Al_{13} (bottom).

the edges of the trigonal prisms. The remaining space is filled by clusters sharing the trigonal prisms with the chain clusters (Figure 10, bottom).

An analysis of the interatomic distances listed in Table 5 reveals that one can generally divide the distances observed in $Co_4Al_{7+x}Si_{2-x}$ into two separate groups: distances which are comparable to or larger than the sum of the atomic radii (r(Al) = 1.43 Å, r(Si) = 1.17 Å, r(Co) = 1.25 Å)[28] and shorter distances which are comparable to the sum of the covalent radii (r(Al) = 1.25 Å, r(Si) = 1.17 Å, r(Co) = 1.16 Å)[28] and thus usually would reflect strong bonding interactions. For example, the Pauling bond order,[33] which is based solely on the interatomic distances, can be calculated according to

$$D(n) = D(1) - 0.6\ \text{Å} \log(n)$$

with $D(n)$ being the bond length in angstroms, $D(1)$ the sum of covalent radii, and n the Pauling bond order. For the observed interatomic distances this suggests a relatively high bond order of 1.17 for d(Co1−Si) = 2.29 Å and 1.21 for d(Co2−Al4) = 2.36 Å. Therefore, we decided to investigate the details of chemical bonding in $Co_4Al_{7+x}Si_{2-x}$.

The electron localization function (ELF) was chosen as the appropriate tool for this investigation. Originally defined by Becke and Edgcombe in the framework of the Hartree−Fock theory[34] and developed later by Savin et al. for density functional theory,[25] the electron localization function belongs to the so-called bonding indicators in real space (i.e., position

(33) Pauling, L. *The Nature of the Chemical Bond*; Cornell University Press: Ithaca, NY, 1948.
(34) Becke, A. D.; Edgecombe, K. E. *J. Chem. Phys.* **1990**, *92*, 5397.

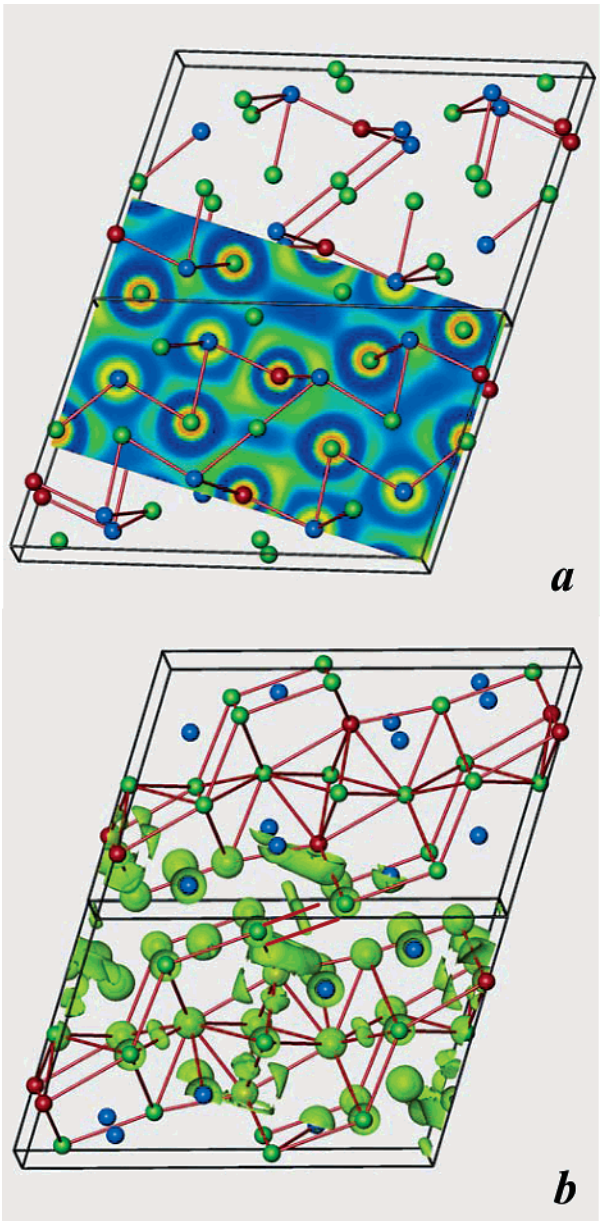

Figure 11. Electron localization function (ELF) in $Co_4Al_{7+x}Si_{2-x}$ (Si, red; Co, blue; Al, green). (a) Section of ELF at $y = 1/2$ and short interatomic distances ($d_{Al-Al} \leq 2.80$ Å; d_{Co-Al}, d_{Co-Si}, $d_{Si-Al} \leq 2.65$ Å); (b) isosurface at $\eta = 0.64$ together with Si−Al and Al−Al bonds.

space).[35] The functions of this group trace the correlation of the electronic motion of same-spin electrons, and a more general function of this type, called the electron localization indicator (ELI), was derived.[36] ELF (as approximation of ELI) represents, in a general sense, a charge distribution of electron pairs and thus is a suitable tool for the analysis of chemical bonding in light of the Lewis theory, where pair formation plays the central role. In the vicinity of the nuclei, ELF and ELI represent the close-shell situation. An even more detailed investigation showed that not only the number of ELF maxima for a given atom but also the integrated electronic population per shell is very close to the values expected from the Aufbau principle.[37] The maxima of ELF

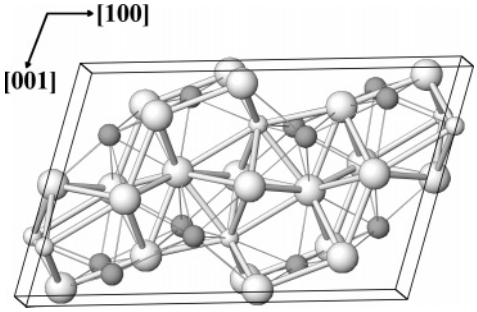

Figure 12. Interatomic interactions in the crystal structure of $Co_4Al_{7+x}Si_{2-x}$, projection along [010]. The covalent Al−Al and Al−Si bonds are shown as sticks, and the rather ionic Co−E interactions are presented as thin lines.

in the valence region (outer shells) provide signatures for directed (covalent) bonding in the position space. The integration of the electron density into the basins of these maxima gives the according electron counts, which allow quantitative description of the bonding situation. Reviews on the application of ELF for different kinds of bonding situations have already appeared.[38]

For $Co_4Al_{7+x}Si_{2-x}$, the section of ELF at $y = 1/2$ (Figure 11a) shows that the inner (core) shells for silicon, aluminum, and cobalt are spherical as it is characteristic for noninteracting atoms.[37] While for Al and Si this is a normal situation, in the case of cobalt the nonstructurized penultimate (3rd) shell suggests that the electrons of this shell do not participate in the interactions in the valence region.[39] This is confirmed by integration of electron density in the 3rd shell giving 15.1 electrons (cf. $3s^23p^63d^7$). Despite the short Co−E distances, the attractors of ELF are not found on these contacts. The maxima of ELF are observed only on the Si−Al or Al−Al bonds (Figure 11b). Thus, from the topology of the electron localization function, chemical bonding in $Co_4Al_{7+x}Si_{2-x}$ can be described as follows. The cobalt atoms transfer two valence electrons of the 4th shell (4s) to the Al/Si network. The silicon and aluminum atoms in the network are covalently bonded. The interaction between cobalt and the network is of a rather ionic nature (Figure 12).

The bonding analysis provides an understanding of the stability of the cluster formed by two trigonal prisms and one rectangular prism in the crystal structures related to $Co_4Al_{7+x}Si_{2-x}$ (Figures 9 and 10). All aluminum (and silicon) atoms occupying the vertexes of the prisms and cubes are covalently bonded and form a part of a 3D polyanion. The cobalt cations are located in the holes of this polyanion.

Conclusions

The crystal structure of $Co_4Al_{7+x}Si_{2-x}$ represents a new type of structure for intermetallic compounds. A partial disorder was found in the vicinity of the 2d site of space group *C*2/*m* which is probably caused by the Si/Al substitution in this part of the crystal structure. This disorder can be resolved by several local ordering models with different Al/

(35) Kohout, M.; Perual, K.; Wagner, F. R.; Grin, Yu. *Theor. Chem. Acc.* **2004**, *112*, 453.
(36) Kohout, M. *Int. J. Quantum Chem.* **2004**, *97*, 651.
(37) Kohout, M.; Savin, A. *Int. J. Quantum Chem.* **1996**, *60*, 875.
(38) Savin, A.; Nesper, R.; Wengert, S.; Fässler, T. F. *Angew. Chem.* **1997**, *109*, 1892.
(39) Kohout, M.; Wagner, F. R.; Grin, Y. *Theor. Chem. Acc.* **2002**, *108*, 150.

Si occupation motifs and different distributions of interatomic distances. The cluster formed by two trigonal prisms around cobalt (transition metal) and a distorted rectangular prism around the Al4 position appears as the common structural motif in the crystal structures of $Co_4Al_{7+x}Si_{2-x}$ and chemically related compounds *o*-Co_4Al_{13} and Fe_4Al_{13}. Different clusters which also contain trigonal prisms around the Co atoms are common for the crystal structures of $Co_4Al_{7+x}Si_{2-x}$ and Os_4Al_{13}. From the analysis of chemical bonding with the electron localization function, the structure can be described as a covalently bonded Al/Si 3D polyanion with rather ionic interactions with cobalt.

Acknowledgment. Financial support from the Austrian science foundation (FWF) under the project number P 14762-PHY is gratefully acknowledged. K.W.R. also thanks the MPG for a research fellowship.

Supporting Information Available: X-ray crystallographic data in CIF format for the structure determination of $Co_4Al_{7+x}Si_{2-x}$. This material is available free of charge via the Internet at http://pubs.acs.org.

IC0401243